Am J Nucl Med Mol Imaging 2022;12(6):166-179
www.ajnmmi.us /ISSN:2160-8407/ajnmmi0147716

Original Article

Comparison of PSMA-based ^{18}F-DCFPyL PET/CT and pelvic multiparametric MRI for lesion detection in the pelvis in patients with prostate cancer

Trinh T Nguyen[1,2], Priya R Bhosale[2], Guofan Xu[1], Tinsu Pan[3], Peng Wei[4], Yang Lu[1]

[1]Department of Nuclear Medicine, Division of Diagnostic Imaging, The University of Texas MD Anderson Cancer Center, Houston, United States; [2]Department of Abdominal Imaging, Division of Diagnostic Imaging, The University of Texas MD Anderson Cancer Center, Houston, United States; [3]Department of Imaging Physics, Division of Diagnostic Imaging, The University of Texas MD Anderson Cancer Center, Houston, United States; [4]Department of Biostatistics, The University of Texas MD Anderson Cancer Center, Houston, United States

Received November 12, 2022; Accepted December 2, 2022; Epub December 15, 2022; Published December 30, 2022

Abstract: Purpose: To directly compare the performance of pelvic mpMRI versus recently approved and increasingly used PSMA-based ^{18}F-DCFPyL PET/CT in intermediate-high risk and biochemical recurrent prostate cancer patient cohort while exploring their potential differing applications in specific clinical scenarios. Methods: A retrospective analysis was performed on patients who had ^{18}F-DCFPyL PET/CT and pelvic mpMRI done from September 2021 to January 2022 at a single institution. The inclusion criteria were paired exams within a 3-month interval. Exclusion criteria were intervening treatment between exams, a change in PSA by more than 50% and absolute difference more than 1 ng/mL, or concurrent history of other malignancy. Abnormal lesions on these 2 imaging exams were reviewed with the identification of concordant and discordant imaging findings. The findings were verified by pathology or other imaging techniques within minimal 5-month clinical follow-up. Results: A total of 57 patients with 57 paired exams were included. The rate of concordant exams was 43/57 or 75.4%. Lesion-based analyses of sensitivity, specificity, PPV and NPV for mpMRI and ^{18}F-DCFPyL PET/CT in the prostate bed were 96%, 94%, 98%, 89% and 96%, 100%, 100%, 90% respectively. For pelvic lymph node metastases, the sensitivity, specificity, PPV and NPV for mpMRI and ^{18}F-DCFPyL PET/CT were 52%, 100%, 100%, 55% and 100%, 100%, 100%, 100% respectively. For bone metastases, the sensitivity, specificity, PPV and NPV for mpMRI and ^{18}F-DCFPyL PET/CT were 86%, 73%, 50%, 94% and 100%, 98%, 95%, 100% respectively. Exact McNemar's test for paired data suggested that in diagnostic performance between ^{18}F-DCFPyL PET/CT and mpMRI was not statistically significant in prostate bed (p-value = 1.00), but significantly in pelvic lymph nodes (p-value < 0.0001) and bone lesions (p-value = 0.0026). Conclusion: Our study demonstrated that PSMA-based ^{18}F-DCFPyL PET/CT and pelvic mpMRI have a good concordance rate in the detection of primary or recurrence prostate disease and can have complementary roles in the clinical assessment of the prostate bed lesions. However, there are key differences in their performance, with the notably superior performance of PSMA-based ^{18}F-DCFPyL PET/CT in the detection of small metastatic nodal disease and bone metastases.

Keywords: PSMA, ^{18}F-DCFPyL, MRI, PET/CT, prostate cancer, metastases

Introduction

Prostate cancer is the second most prevalent cancer in men worldwide, the most common cancer in men and third leading cause of death in the United States [1]. Given its typically indolent course and decreasing trend in overutilization of prostate-specific antigen (PSA) screening, the incidence of metastatic prostate cancer is rising [2]. Management of prostate cancer has become progressively reliant on diagnostic imaging as advances are made in the field of radiological imaging. Of which, prostate-specific membrane antigen (PSMA)-based PET/CT and multiparametric MRI have taken the leading roles in primary staging of prostate cancer and evaluation for recurrent disease.

PSMA is a type II transmembrane glycoprotein that is frequently overexpressed in prostate cancer, a variety of non-prostate cancers and normal endothelial cells [3-6]. Currently,

^{68}Ga-PSMA-11 and ^{18}F-DCFPyL (PYLARIFY) are the only 2 PET/CT agents approved by the FDA for patients with prostate cancer. Based on the landmark OSPREY trial [7], which demonstrated high diagnostic accuracy of the novel radiotracer ^{18}F-DCFPyL PET/CT for detection of prostate cancer and metastases, in May 2021 the FDA had approved the use of ^{18}F-DCFPyL PET/CT for initial staging of patients with suspected metastatic prostate cancer as well as those with concern for recurrent disease. The ^{18}F-DCFPyL is a second-generation low molecular weight radiofluorinated PSMA-targeted PET radiotracer. Given its easier commercial availability, more flexibility in scheduling patients due to its longer half-life than ^{68}Ga-PSMA-11, favorable safety profile, stable biodistribution, and high lesion-to-background contrast which results in increased diagnostic confidence, ^{18}F-DCFPyL has quickly gained significant popularity in routine clinical use shortly after its approval.

Conversely, multiparametric MRI (mpMRI) is a well-established modality in prostate cancer workup, readily available at many institutions. Given the intrinsic high tissue contrast of mpMRI, it offers excellent spatial resolution and clear delineation of anatomical structures for primary prostate cancer lesions, including marginal invasion of surrounding structures such as the rectum and bladder, which are less easily discerned in PET/CT. However, the diagnostic performance for regional and distant metastases between these modalities is expected to differ. Few studies have quantified these variances, which were mainly based on ^{68}Ga-PSMA-11 and mpMRI comparison [8-13]. There is very limited data with intraindividual comparison of pelvic mpMRI and ^{18}F-DCFPyL PET/CT. With the increasingly widely used ^{18}F-DCFPyL over ^{68}Ga-PSMA-11 for PSMA-based PET/CT in clinical practice, there is unmet and substantial interests in understanding the diagnostic utility of ^{18}F-DCFPyL PET/CT versus pelvic mpMRI in prostate cancer. Our retrospective study assesses the performance of these two imaging tools in the settings of intermediate-high risk de-novo prostate cancer and suspected recurrence in previously treated patients.

Methods

Patient selection

An institutional review board approved retrospective study was performed on prostate cancer patients who had ^{18}F-DCFPyL PET/CT and mpMRI performed from 9/1/2021 to 1/31/2022. The selected cohort included patients with intermediate-high risk prostate cancer and those with biochemical recurrence. The patients were included if they underwent the paired exams within a 3-month interval. Exclusion criteria were intervening treatment between the PET and MRI exams, a change in PSA by more than 50% between exams and absolute difference in PSA level of more than 1 ng/ml, or concurrent history of other malignancy. Exams of poor quality or lacking key MRI imaging sequences were eliminated from the analysis.

^{18}F-DCFPyL PET/CT protocol

Our institutional ^{18}F-DCFPyL PET/CT protocol is in keeping with the OSPREY trial [7] and FDA approved PYLARIFY package insert. In brief, patients fasted, except for water, for at least 4 hours before injection of approximately 333 MBq (9 mCi) of ^{18}F-DCFPyL. At 60-90 minutes following the injection, PET/CT imaging was performed from the skull to the mid-thigh. All PET/CT were performed on integrated PET/CT scanners, either on a GE 64-slice Discovery 710 PET/CT scanner, or GE discovery MI 64slice PETCT (GE Healthcare, Waukesha, Wisconsin, USA) or a Siemens 64-slice Biograph mCT PET/CT scanner (Siemens Medical Systems, Erlangen, Germany) using institutional standard protocol. Low-dose CT was performed with tube-current modulation with intravenous contrast.

Pelvic mpMRI protocol

All imaging studies were performed with an endorectal coil using either 1.5T or 3.0T magnets, or without an endorectal coil using 3T magnets, following a standard institutional protocol. The sequences included are 3-plane localizer, 3-plane small field-of-view (FOV) T2, axial T1 small FOV, axial Diffusion weighted imaging (DWI) small FOV, whole pelvis axial T1 pre-contrast, whole pelvis axial DWI, and small FOV axial 3D Dynamic contrast enhancement (DCE).

Image interpretation

For each eligible patient, we compared the lesions included in the pelvis FOV of the mpMRI and the PET/CT. Images of ^{18}F-DCFPyL PET/CT and mpMRI were re-reviewed by all investiga-

Table 1. Patient clinical characteristics

Age (years)	
Median	67
Range	50-84
Total Gleason Score (Highest grades)	Patients (N = 57)
10	1
9	19
8	8
7	25
6	3
Unknown	1
PSA at PET (ng/ml)	
Median	3.2
Range	< 0.1-71.7

tors with blind to the original reports and classified as concordant or discordant. The initial interpretation of the ^{18}F-DCFPyL PET/CT was performed by a group of 10 board certified nuclear medicine physicians. The initial interpretation of pelvic mpMRI was performed by a group of 40 board certified and fellowship trained body radiologists proficient in the Prostate Imaging Reporting and Data System (PI-RADS) v2.1 reporting methodology as established by the American College of Radiology.

Independent re-analysis was performed by two fellowship-trained abdominal imaging radiologists and two nuclear medicine trained radiologists who were blinded to clinical information and other imaging. The two abdominal radiologists (TN and PB) have 5 and 22 years of MRI interpretation, respectively, while the two nuclear medicine radiologists (YL and GX) both have over 10 years of experience in PET imaging interpretation.

The review of mpMRI studies include assessment of significant lesions in the prostate bed, local organ involvement, pelvic nodal metastases, and skeletal metastases. Evaluation of prostate bed lesions include assignment of a likert or PI-RADS score for likelihood of a clinically significant lesion. A likert or PI-RADS score of 4 or 5 in the prostate bed were considered positive. Meanwhile, the assessment of nodal metastases was largely based on nodal size, morphology, and asymmetry. Asymmetrically enlarged lymph nodes with abnormal morphology such as round configuration and heterogeneous signal were typically considered positive. In general, pelvic lymph nodes with short axis less than 8 mm were considered negative unless atypical MRI morphologic features were present. Equivocal lymph nodes were also noted in data collection and considered negative in data analysis. Likewise, abnormal skeletal lesions were identified on mpMRI and considered positive in data analysis. Identification of equivocal lesions was made and considered negative in the statistical analysis.

On ^{18}F-DCFPyL PET/CT scans, any lesion with distinct, nonphysiological focal tracer uptake higher than adjacent normal soft tissue background was counted as positive.

Pelvic lesion-based comparison was made among every investigator's independent review result and original reports. Any positive and discrepancy imaging findings among investigators, or discrepancy with original reports were discussed and independently assessed by board certified and fellowship trained body radiologist and nuclear medicine physician. Consensus among investigators was reached after this subsequent review and minimal 5 months follow-up till June 30, 2022, based on all the available imaging, pathology, and clinical data. Corresponding patient, tumor characteristics and PSA levels within 30 days of PET/CT or MRI from electronic medical records were recorded.

Statistical analysis

Pelvic lesion-based comparison of the two imaging modalities was performed by a two-sided exact McNemar test [14]. A p value of < 0.05 was considered statistically significant. Exact 95% confidence intervals (CIs) were calculated for diagnostic performance measures including sensitivity, specificity, positive predictive value (PPV) and negative predictive value (NPV). Analysis was performed using statistical software R (version 4.2.1) and Excel for Microsoft 365.

Results

A total of 57 patients with 57 eligible paired exams were analyzed. The median age of the patient cohort was 67 years (range, 50-84). The Gleason scores and PSAs within 30 days of MRI and ^{18}F-DCFPyL PET/CT exam were documented. The median PSA near the time of ^{18}F-DCFPyL PET/CT was 3.2 ng/mL, range of < 0.1-71.7 ng/mL. The patient's clinical characteristics were summarized in **Table 1**. The

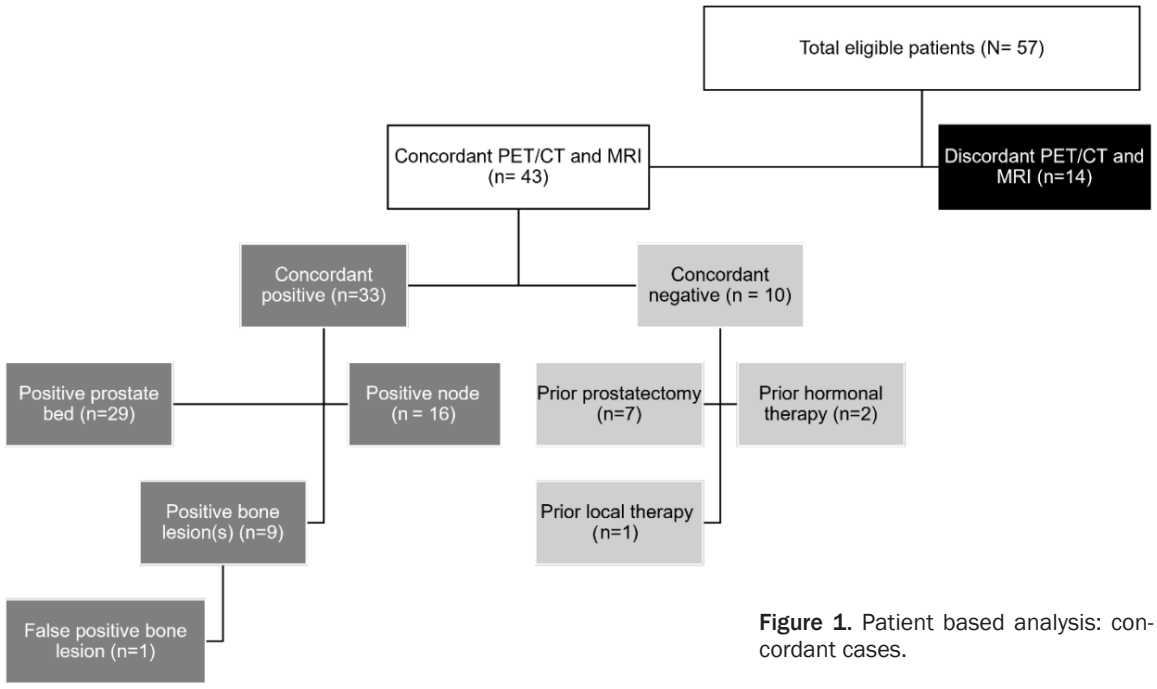

Figure 1. Patient based analysis: concordant cases.

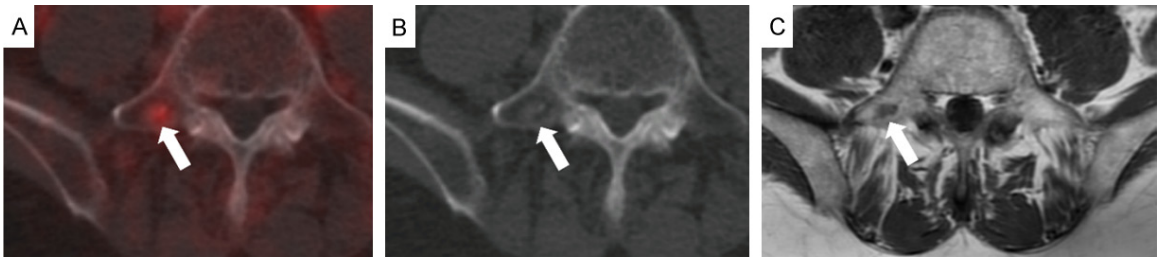

Figure 2. A 66-year-old man with Gleason 7 (4+3) prostate adenocarcinoma underwent radical prostatectomy and pelvic bilateral lymph nodes dissection, with positive margin and 1/31 positive lymph node, presented with postop rising PSA to 0.2 ng/ml. ^{18}F-DCFPyL PET/CT (A: Fused axial ^{18}F-DCFPyL PET/CT; B: Axial CT) showed a PSMA avid sclerotic focus in right L5 transverse process (arrows in A & B, SUVmax 3), with concordant abnormal findings on mpMRI with low T1 signal (arrow in C: Axial T1 MRI). However, the lesion was later biopsy confirmed as benign.

paired studies were considered concordant if there is no discrepancy between MRI and ^{18}F-DCFPyL PET/CT findings, and discrepant if there were any differences in findings regarding the prostate bed, pelvic organs, nodal or skeletal metastases. **Figure 1** illustrates the breakdown of concordant and discordant cases.

Patient-based analysis

Analysis of concordant cases: As demonstrated in **Figure 1**, ^{18}F-DCFPyL PET/CT and mpMRI have a good degree of concordance (43/57 or 75.4%). Among the concordant cases, 10 paired exams demonstrated concordant negativity.

Of the concordant positive paired exams (n = 33), 29/33 (87.9%) demonstrated disease in the prostate bed, 16/33 (48.9%) demonstrated positive pelvic nodal disease, and 9/33 (27.3%) demonstrated positive pelvic bone lesion(s). It was also noted that one concordant paired exam demonstrated a false positive skeletal lesion that was confirmed on biopsy (**Figure 2**).

Analysis of discordant cases: An analysis of the discordant paired exams (n = 14) was performed stratified by the treatment status (**Figure 3**).

Of the 2 patients who have not been treated for prostate cancer (n = 2), 1 case of false negative

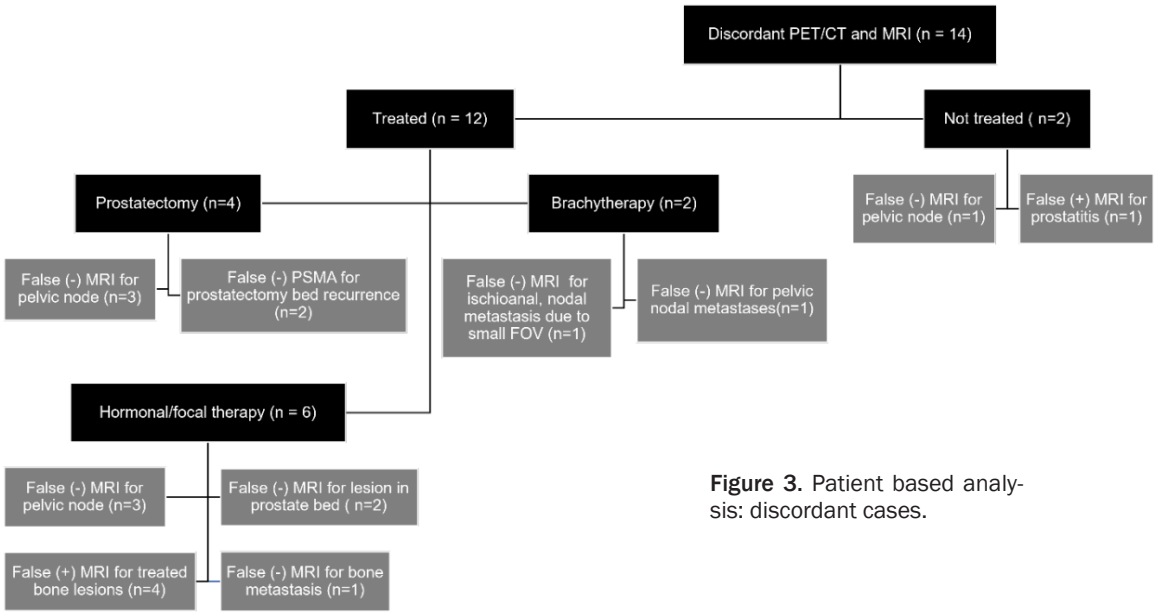

Figure 3. Patient based analysis: discordant cases.

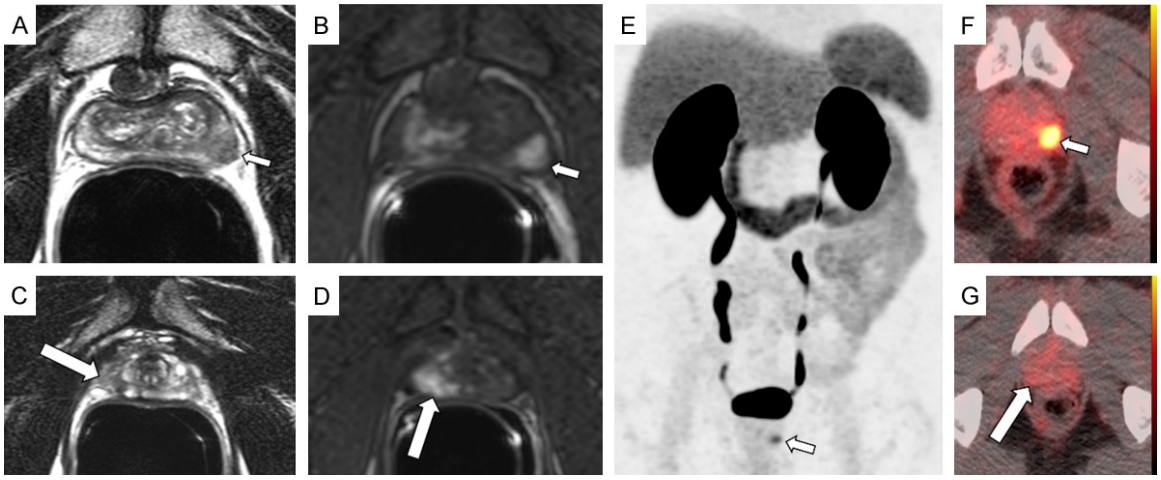

Figure 4. A 66-year-old man with recent outside institution diagnosis of prostate cancer had abnormal findings on pelvic mpMRI (A & C: Axial T2 MRI; B & D: Axial T1 post contrast MRI); showing low T2 signal intensity and enhancing lesions in left base peripheral zone (short arrows in A & B, measures about 1.3 × 1.2 cm) and right apical peripheral zone (long arrows in C & D, measures about 1.8 × 1 cm). The patient underwent a ^{18}F-DCFPyL PET/CT (E: ^{18}F-DCFPyL PET MIP; F & G: Fused axial ^{18}F-DCFPyL PET/CT) 5 days later with PSA of 3.8 ng/ml at time of ^{18}F-DCFPyL PET/CT. The ^{18}F-DCFPyL PET/CT showed PSMA avid lesion in the left peripheral zone (short arrows in E & F, SUVmax 6.8), but not the right apical lesion seen on mpMRI (long arrow in G, with background uptake of SUVmax 2.8). Biopsy confirmed the Gleason 7 (4+3) prostate adenocarcinoma in left peripheral zone (short arrows in A, B, E, F), but prostatitis in right apical gland (long arrows in C, D, G).

MRI for pelvic nodal disease and 1 case of false positive MRI due to underlying prostatitis (**Figure 4**) were identified.

Of patients with prior prostatectomy (n = 4), 3 cases had false negative MRI for pelvic nodal disease and 2 cases had false negative ^{18}F-DCFPyL PET/CT for recurrence in the prostatectomy bed. One representative case was shown in **Figure 5**.

Of patients who underwent prior brachytherapy treatment (n = 2), we identified 1 case of false negative MRI for nodal metastasis in the left

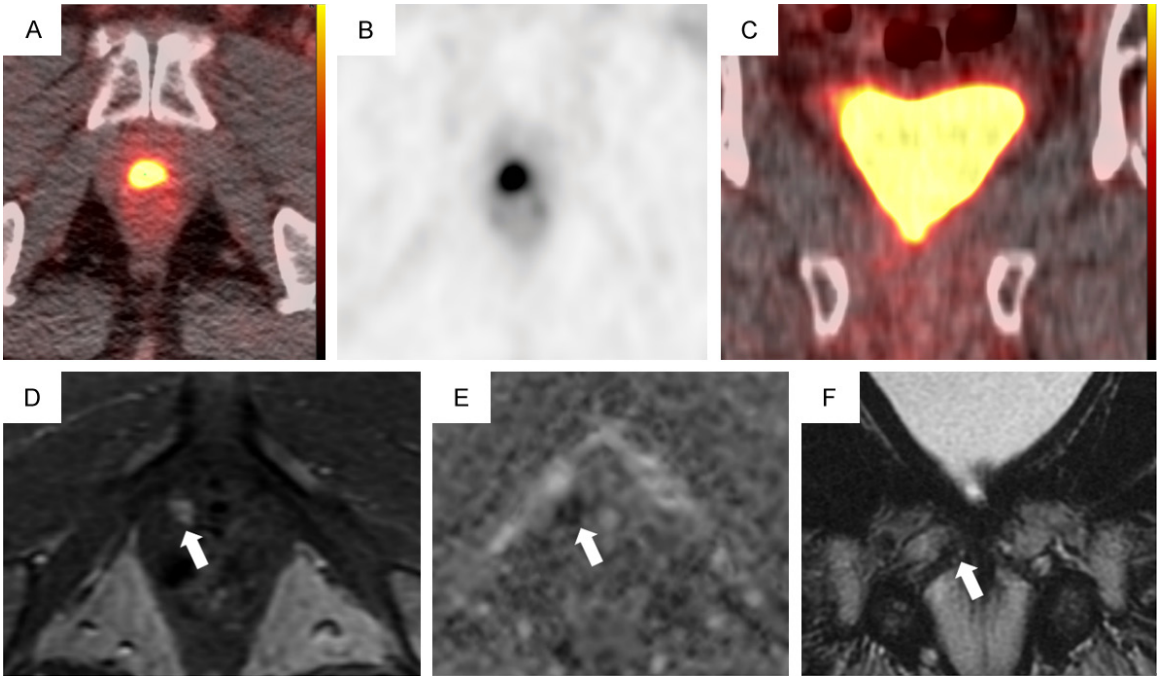

Figure 5. A 64-year-old man with Gleason 8 (4+4) prostate adenocarcinoma, status post prostatectomy with post-operative rising PSA of 2.4 ng/mL on the day of ^{18}F-DCFPyL PET/CT (A: Fused axial ^{18}F-DCFPyL PET/CT; B: Axial ^{18}F-DCFPyL PET; C: Fused coronal ^{18}F-DCFPyL PET/CT) and pelvic mpMRI (D: Axial T1 post contrast MRI; E: Axial ADC MRI; F: Coronal T2 MRI). The ^{18}F-DCFPyL PET/CT didn't reveal any suspicious lesion, while the same day mpMRI revealed a 1 cm focus to the right of the vesicourethral anastomosis showing abnormal enhancement (arrow in D), with mild restricted diffusion (arrow in E) and low T2 signal (arrow in F), suggestive of tumor recurrence. The focus couldn't be identified at retrospective analysis of the ^{18}F-DCFPyL PET/CT, partially due to the intense urinary activity in this region (A-C).

peri-anal ischioanal fossa region due to small field of view and 1 case of false negative MRI for multiple pelvic nodal metastasis (**Figure 6**).

Of patients with prior hormonal and/or focal therapy (n = 6), 3 cases had false negative MRI for pelvic nodal disease, 4 cases had false positive MRI for treated metastatic bone lesion (representative case shown in **Figure 7**), 1 case had false negative MRI for bone metastasis (**Figure 8**), and 2 case had false negative MRI for residual disease in the prostate bed with one of the 2 cases showed false negative MRI for both prostate bed and pelvic lymph node (**Figure 9**).

Lesion-based analysis

On lesion-based comparison analysis, we categorized the positive lesions into 3 groups: prostate bed, pelvic lymph nodes and bone lesions. The direct extraprostatic extension, neurovascular invasion, local organ invasion, as well as seminal vesicle lesions were counted into prostate bed lesions. There was a total of 54 lesions deemed as true positive in the prostate bed, 62 metastatic pelvic lymph nodes and 21 pelvic bone metastases.

Table 2 contains statistical analysis of mpMRI and ^{18}F-DCFPyL PET/CT diagnostic performance. In prostate bed, the mpMRI had a sensitivity of 96% (95% CI: 87%-100%), specificity of 94% (95% CI: 73%-100%), PPV of 98% (95% CI: 90%-100%), NPV of 89% (95% CI: 67%-99%); the ^{18}F-DCFPyL PET/CT had a sensitivity of 96% (95% CI: 87%-100%), specificity of 100% (95% CI: 81%-100%), PPV of 100% (95% CI: 93%-100%), NPV of 90% (95% CI: 68%-99%).

In pelvic lymph nodes, the mpMRI had a sensitivity of 52% (95% CI: 39%-65%), specificity of 100% (95% CI: 91%-100%), PPV of 100% (95% CI: 89%-100%), NPV of 55% (95% CI: 43%-67%); the ^{18}F-DCFPyL PET/CT had a sensitivity of 100% (95% CI: 94%-100%), specificity of 100% (95% CI: 91%-100%), PPV of 100% (95% CI: 94%-100%), NPV of 100% (95% CI: 91%-100%).

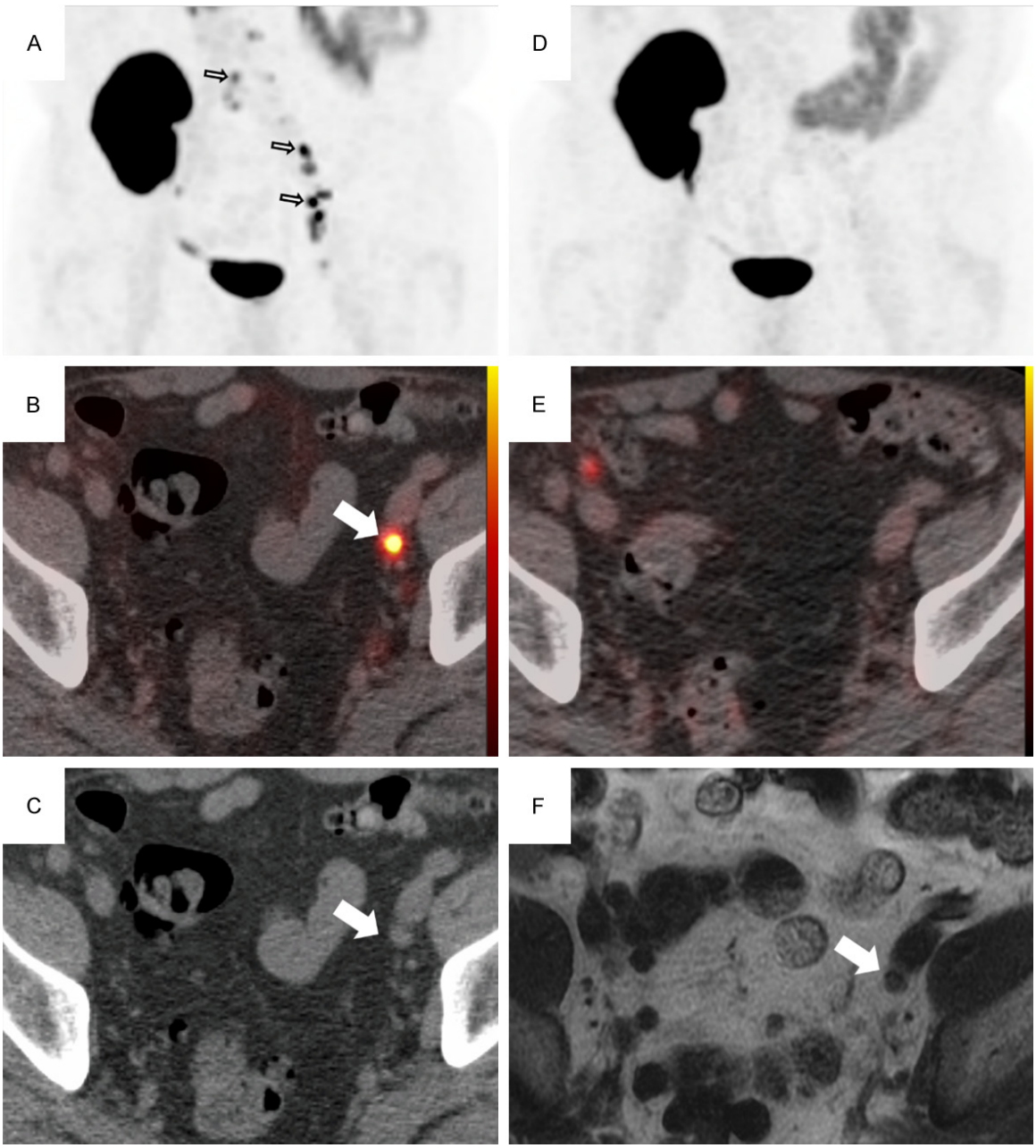

Figure 6. A 75-year-old man with Gleason 7 (3+4) prostatic adenocarcinoma, had history of renal transplant, received brachytherapy. His PSA was 9.5 ng/mL one day prior to ^{18}F-DCFPyL PET/CT (A: ^{18}F-DCFPyL PET MIP; B: Fused axial ^{18}F-DCFPyL PET/CT; C: Axial CT). ^{18}F-DCFPyL PET/CT showed multiple PSMA-avid subcentimeter pelvic lymphoadenopathy along the iliac chains, more on the left (small arrows in A). A representative 0.6 cm left external iliac lymph node with intense PSMA avidity (block arrows in B & C, SUVmax 23.4). These lymph nodes resolved at a 7-month follow up ^{18}F-DCFPyL PET/CT (D: MIP; E: Fused axial PET/CT), when PSA dropped to < 0.1 ng/mL. The subcentimeter pelvic lymph nodes had normal appearance on the concurrent pelvic mpMRI of the first ^{18}F-DCFPyL PET/CT, including the left external iliac lymph node (block arrow in F: Axial T1 MRI).

In bone lesions, the mpMRI had a sensitivity of 86% (95% CI: 64%-97%), specificity of 73% (95% CI: 60%-83%), PPV of 50% (95% CI: 33%-67%), NPV of 94% (95% CI: 84%-99%); the ^{18}F-DCFPyL PET/CT had a sensitivity of 100% (95% CI: 84%-100%), specificity of 98% (95% CI: 92%-100%), PPV of 95% (95% CI: 77%-100%), NPV of 100% (95% CI: 94%-100%).

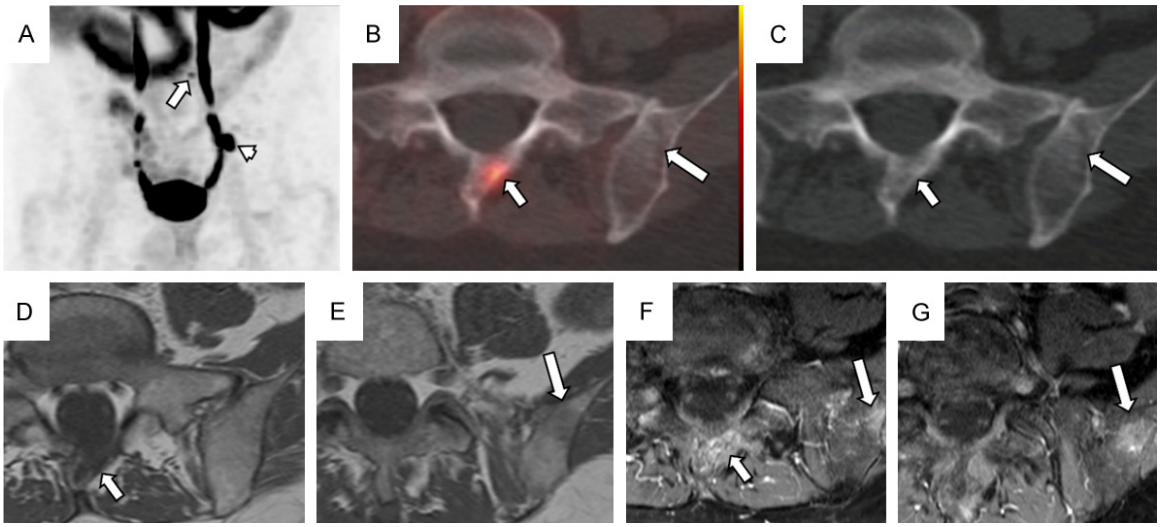

Figure 7. A 69-year-old man with Gleason 7 (3+4) prostatic adenocarcinoma had cryoablation and was on leuprolide and apalutamide. He had rising PSA of 2.4 ng/mL two days prior to ^{18}F-DCFPyL PET/CT (A: ^{18}F-DCFPyL PET MIP; B: Fused axial ^{18}F-DCFPyL PET/CT; C: Axial CT). Besides a known pelvic lymph node metastasis (arrowhead in A) being PSMA avid, a sclerotic left L5 lesion (short arrows in A-C) showed PSMA avidity (SUVmax 5), while another sclerotic focus in left posterior iliac bone was non-PSMA avid (long arrows in B & C). Both lesions showed low T1 signal and enhancement on pelvic mpMRI (D & E: Axial T1 MRI; F & G: Axial T1 post contrast MRI) performed 30 days later when PSA rose to 3.2 ng/mL and were interpreted as being positive when blinded with ^{18}F-DCFPyL PET/CT and medical information. The L5 lesion was deemed as true positive (short arrows in D & F), while the left iliac bone lesion being false positive (long arrows in F, G) on mpMRI.

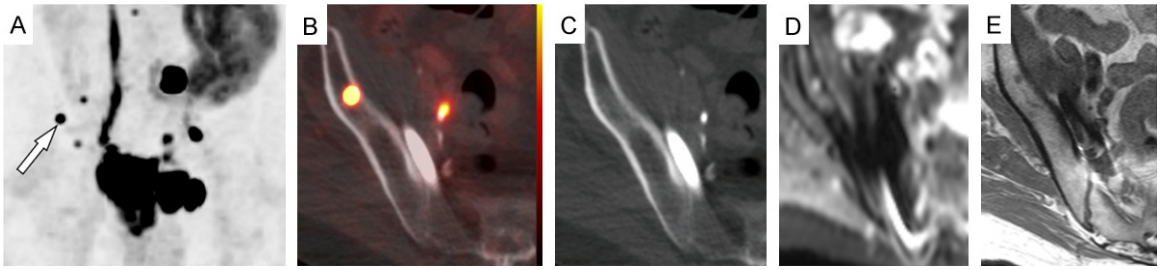

Figure 8. An 84-year-old man with Gleason 9 (4+5) prostate adenocarcinoma had known multiple bone metastasis and was on therapy with abiraterone/prednisone. His PSA dropped from 3.51 ng/mL to 1.7 ng/mL in 2 months at time of ^{18}F-DCFPyL PET/CT (A: ^{18}F-DCFPyL PET MIP; B: Fused axial ^{18}F-DCFPyL PET/CT; C: Axial CT) and mpMRI (D: Axial DWI MRI; E: Axial T1 MRI). The bone metastases were PSMA avid (short and long arrows in A), but 3 small PSMA avid lesions were missed on mpMRI, including a subtle sclerotic lesion in the right iliac bone (SUVmax 33.6, long arrows in A-E). Retrospectively, the right iliac bone lesion measured about 4 mm on mpMRI with high signal on DWI with restriction diffusion (long arrows in D) and low T1 signal (long arrow in E), suggestive for bone metastasis.

Exact McNemar's test for paired data suggested that in diagnostic performance between ^{18}F-DCFPyL PET/CT and MRI was not statistically significant in prostate bed (p-value = 1.00), but significantly in pelvic lymph nodes (p-value < 0.0001) and bone lesions (p-value = 0.0026).

Discussion

Over the years, mpMRI has been widely accepted for its accuracy and specificity in the detection of clinically significant prostate cancer in patients who have not been treated, thereby lowering the rate of unnecessary biopsy. With high tissue contrast, mpMRI is highly accurate in the primary staging of prostate cancer and characterization of the local disease extent. Some studies have demonstrated the superior performance of mpMRI to ^{68}Ga-PSMA PET/CT in the setting of low-intermediate risk prostate cancer [15]. MpMRI is also indicated in the setting of suspected local recurrence after prostatectomy, biochemical recurrence after radia-

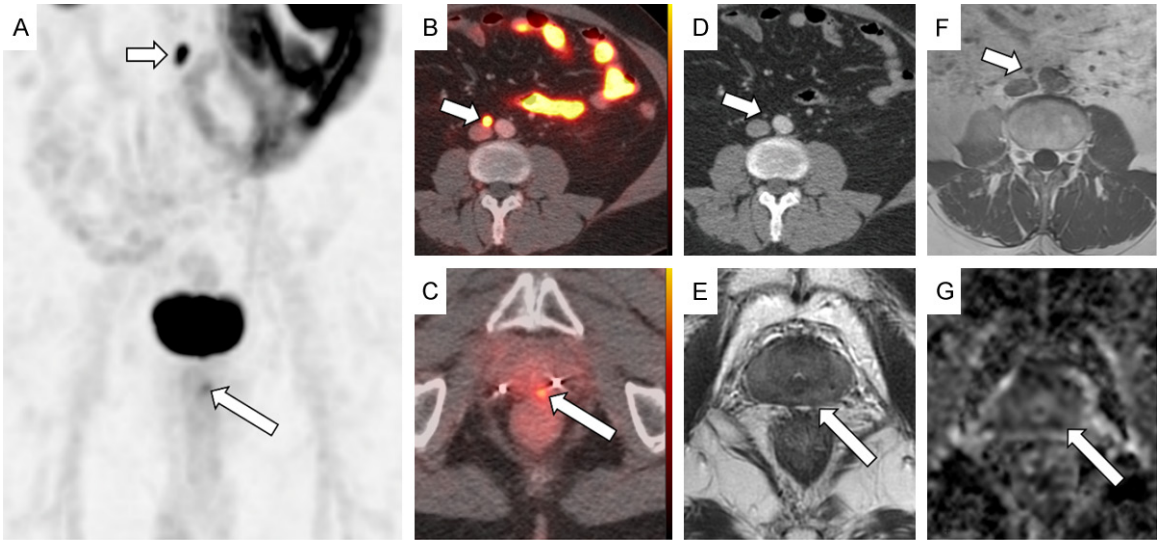

Figure 9. A 58-year-old man with Gleason 7 (3+4) prostatic adenocarcinoma treated with leuprolide, abiraterone and radiation. He had rising PSA of 2.9 ng/mL on the same day of ^{18}F-DCFPyL PET/CT (A: ^{18}F-DCFPyL PET MIP; B & C: Fused axial ^{18}F-DCFPyL PET/CT; D: Axial CT) and mpMRI (E: Axial T2 MRI; F: Axial T1 MRI; G: Axial ADC MRI). A PSMA avid 0.4 cm interaortacaval LN at level of bifurcation (SUVmax 14.7, short arrows in A, B & D) appeared as normal on mpMRI (short arrow on F). The PSMA avid tumor recurrence in the left paramidline peripheral zone (SUVmax 5.7, long arrows in A & C), was missed on mpMRI but retrospectively correlated a subcentimeter lesion with low T2 signal (long arrow in E) and diffusion restriction (long arrow in G), suggestive for malignancy.

Table 2. Lesion based pelvic mpMRI and ^{18}F-DCFPyL PET/CT diagnosis performance

		Recurrence/Metastases+		Recurrence/Metastases-	
		MRI+	MRI-*	MRI+	MRI-
Prostate Bed	PET/CT+	50	2	0	0
	PET/CT-	2	0	1	17#
Lymph nodes	PET/CT+	32	30	0	0
	PET/CT-	0	0	0	37#
Bone	PET/CT+	18	3	1	0
	PET/CT-	0	0	17	48#

*: Including the intermediate/equivocal lesions on mpMRI, which were analyzed as negative. #: Indicating the number of patients with negative findings.

tion therapy, and can be used to guide targeted biopsy using MRI/US fusion technology. However, the diagnostic performance of mpMRI may be decreased in the post-treatment setting due to therapy-induced morphologic and dynamic functional changes [16].

Currently, majority of the published clinical PSMA-based PET/CT studies are based on ^{68}Ga-PSMA-11 PET/CT. Many studies showed the efficacy of PSMA PET/CT in the restaging of disease, with up to > 90% sensitivity if PSA is > 1 ng/mL [17]. PSMA-based PET/CT has the added theranostic benefit of being coupled with lutetium-177 PSMA targeted therapy in patients with metastatic castrate-resistant prostate cancer [18]. Some limitations of PSMA include false positivity from normal ganglia and neovasculature of other tumors or benign etiologies [4]. Additionally, some prostate cancers are non-PSMA producing such as poorly differentiated carcinomas and those with neuroendocrine dedifferentiation, therefore not well-detected by PSMA-based PET/CT [19]. Since the recent FDA approval, PSMA-based ^{18}F-DCFPyL PET/CT has been increasingly used in routine clinical practice for the evaluation of prostate cancer. Given its satisfying imaging quality, commercial availability, and favorable technical profile, ^{18}F-DCFPyL PET/CT has gain

popularity over ^{68}Ga-PSMA-11 PET/CT. However, due to its infancy stage of clinical use, little is known regarding its diagnostic performance over other well-established imaging modalities, such as pelvic mpMRI.

Our study demonstrated ^{18}F-DCFPyL PET/CT and mpMRI have a fairly good degree of concordance on patient-based analysis (43/57, 75.4%). Of the 14/57 (24.6%) discordant cases, 10 cases had false negative MRI for subcentimeter pelvic nodal metastases, indicating limited sensitivity of MRI for subcentimeter nodal disease. Further lesion-based analysis of the discordant cases showed unique differences in the performance of these two imaging techniques. The ^{18}F-DCFPyL PET/CT demonstrated significant higher sensitivity in detecting pelvic lymph node metastases, especially in the subcentimeter sized lymph nodes. For bone metastasis, ^{18}F-DCFPyL PET/CT showed better capacity in differentiating treated versus active metastasis (**Figure 7**).

For primary lesion detection in the prostate bed, although the two imaging modalities showed similar diagnostic performance in our patient cohort, it is generally thought that mpMRI has intrinsic advantage in soft tissue anatomic evaluation over PET/CT, especially regarding the intra- and extra-prostatic disease extent, local invasion of the rectal and bladder wall, neurovascular bundle, and seminal vesicles. However, ^{18}F-DCFPyL PET/CT may have increased specificity in the detection of significant prostate cancer in patients who have not been treated. As seen in **Figure 4**, mpMRI identified a lesion in the right prostate apex, prospectively deemed as a PI-RADS 4 lesion, discordant with PET/CT findings. A retrospective evaluation with pathologic correlation revealed that this was focal prostatitis mimicking a prostate malignant lesion, resulting in a false positive mpMRI. This suggests superior specificity of PSMA PET/CT to mpMRI in the detection of clinically significant disease in untreated patients. In the primary staging of intermediate-high risk patients, this argues that PSMA PET/CT may have a complementary role and increase diagnostic accuracy.

In our study cohort, of the patients who had a prior prostatectomy in the discordant group (n = 4), 2/4 patients had false negative ^{18}F-DCFPyL PET/CT for recurrence in the prostatectomy bed. As shown in **Figure 5**, the intense urinary activity on ^{18}F-DCFPyL PET/CT limited the evaluation of early recurrence in prostate bed. And recurrence was only seen on mpMRI in vesicourethral junction in prostatectomy bed. As previously described in the literature, recurrent disease post-prostatectomy is most commonly seen at the vesicourethral anastomosis [20], and often only detected on post-contrast sequence MRI [21]. Thus, mpMRI may be superior to PSMA-based ^{18}F-DCFPyL PET/CT for the detection of local recurrence in the prostatectomy bed in the setting of rising PSA but negative findings on ^{18}F-DCFPyL PET/CT. Alternatively, another FDG-approved PET tracer Fluciclovine PET/CT would help in this scenario due to its minimal to none urinary activity [22].

Conversely, we identified PSMA avid early recurrence on ^{18}F-DCFPyL PET/CT which was deemed as negative on mpMRI due to post-treatment change from external beam radiation (**Figure 9**), or brachytherapy. As previously demonstrated in other studies, post-therapeutic changes from focal therapy can limit the assessment of recurrence due to induction prostatic architectural changes that overlap with tumor appearance [23]. Hormonal therapy can induce glandular atrophy and decrease glandular vascularity, making interpretation more difficult [24]. Metallic brachytherapy capsules can induce significant susceptibility artifacts, distorting the DWI sequence and therefore limiting the evaluation of recurrence in the prostate bed [25].

On the other hand, false positive mpMRI is not uncommon in the post-brachytherapy setting as a result of prostatitis, hemorrhage, or dysplasia [26]. Effectively, PSMA-based ^{18}F-DCFPyL PET/CT may play a crucial role in the detection of recurrence in the prostate gland in these specific clinical settings. Review of literature demonstrates inter-reader variability with modest sensitivity of mpMRI for detection of recurrence in the post-brachytherapy setting [27]. Additionally, the accuracy of mpMRI is lower in post low-dose-rate brachytherapy versus high-dose-rate brachytherapy [27]. This again underscores the limited role of mpMRI in the post-treatment setting and suggests that PSMA may have a preferred role in the detection of recurrence post brachytherapy.

As expected, there is a high degree of uncertainty for the detection of nodal pathology with MRI. Using widely adopted size threshold (8 mm in short axis) or asymmetry, we missed a significant number of cases with metastatic pelvic lymph nodes in 10 patients (10/57), especially those subcentimeter lymph node metastases. As shown in **Figure 6**, a patient with many PSMA positive subcentimeter lymph node metastases were missed on mpMRI. MRI diagnostic confidence is increased when the lymph node is obviously enlarged, abnormal in morphology, or asymmetrically prominent, however, the sensitivity remains suboptimal. PSMA-based PET/CT is significantly more sensitive than MRI for the detection of pathologic nodal disease because of its high lesion-to-background contrast. Our study demonstrates that PSMA-based ^{18}F-DCFPyL PET/CT can detect lymph nodes as small as 0.4 cm.

In the same discordant group of patients previously treated with brachytherapy (n = 2), we identified a case of false negative mpMRI for nodal metastasis in the left peri-anal ischioanal fossa region, but positive on ^{18}F-DCFPyL PET/CT and was later confirmed through biopsy. Retrospective MRI evaluation shows that the 1 cm lesion could only be seen in the large field-of-view Axial T1 and T2 sequences, and was not included in DWI and dynamic post-contrast imaging sequences due to smaller FOV. This demonstrates inherent blind spots associated with the MRI technique, in which the reader may only focus on the anatomy within the small FOV sequences and neglect other anatomic regions on certain sequences. The large number of sequences required for interpretation using mpMRI with variable FOVs may detract the reader from maintaining focus and accuracy.

In the setting of treated skeletal metastases, mpMRI can effectively identify skeletal lesions but is unable to distinguish their biological activity, specifically whether the disease is still active and requires continued treatment or change in therapy. Conversely, PSMA-based ^{18}F-DCFPyL PET/CT can characterize the lesions in terms of their functional activity status, which may play a more crucial role in guiding therapy. In **Figure 7**, both the left S1 lamina and left iliac bone lesions showed low T1 signal and enhancement on mpMRI, and were deemed as suspicious for prostate metastases on mpMRI. However, the PSMA avidity confirms a functional active prostate cancer. In the same patient, additional bone lesions were identified without PSMA avidity and retrospectively deemed as treated disease.

Interestingly, of our 33 concordant positive paired exams, we identified a case of concordant false positive bone lesion on both ^{18}F-DCFPyL PET/CT and mpMRI, as demonstrated in **Figure 2**. The L5 lesion was subsequently biopsy confirmed as benign. This highlights the limitations of both imaging modalities. While mpMRI can detect abnormal skeletal lesions, it has limited specificity for distinguishing benign vs. malignant nature, specifically in small lesions such as the one depicted in this example. Conversely, ^{18}F-DCFPyL PET/CT is highly sensitive and specific for the detection of lesions characteristic of prostate metastases, however, it is susceptible to false positive results, as previously described in the literature [28]. Some PSMA avid skeletal mimics of prostate metastases include fractures, osteomyelitis, fibrous dysplasia, Paget's disease, or other malignant metastases [28].

In the 10 paired exams of concordant negativity, with corresponding PSAs ranging from 0.2-2.2 ng/mL. Of this group, we identified a disproportionate number of cases with a history of prior radical prostatectomy, 7/10 patients. Of the remaining cases, 2/10 patients were previously treated with hormonal therapy and 1/10 patient underwent prior external beam radiation therapy. It is puzzling whether the concordant negativity is due to low PSA levels or suggest inherent limitations of both imaging modalities in the detection of recurrent disease in biochemical recurrent patients, especially post-prostatectomy patients. More research in this specific population with fine-tuning of imaging techniques would provide more insights.

Some limitations of our study include those inherent of a single-center retrospective analysis. It is worth noting that our patient cohort may represent a selection bias as only intermediate-high risk patients and previously treated patients with biochemical recurrence were included, partially due to our referring medical oncologists' practice preference. Further large cohort prospective studies to include low-risk category patients may offer more evidence on the overall performance of PSMA-based

^{18}F-DCFPyL PET/CT versus mpMRI. Additionally, it is impossible and unrealistic to confirm every positive lesion with histopathology.

Conclusion

Our retrospective analysis from the intermediate-high risk and biochemical recurrent patient cohort, showed PSMA-based ^{18}F-DCFPyL PET/CT has better diagnostic performance in detecting metastatic nodal and bone disease. ^{18}F-DCFPyL PET/CT is superior than mpMRI in detecting subcentimeter lymph node metastases, and differentiating treated versus active metastatic bone lesions.

Although no significant difference in diagnostic performance in detecting disease in prostate bed, ^{18}F-DCFPyL PET/CT and pelvic mpMRI may have complementary benefits depending on specific clinical scenarios. The mpMRI has intrinsic advantage in soft tissue anatomic evaluation over PET/CT, especially regarding the intra- and extra-prostatic disease extent. Additionally, mpMRI may be superior to PSMA-based ^{18}F-DCFPyL PET/CT for the detection of local recurrence in the prostatectomy bed in the setting of rising PSA but negative PET/CT findings. However, ^{18}F-DCFPyL PET/CT may further differentiate prostate cancer from mimics such as prostatitis, post treatment changes from prior brachytherapy, hormonal, and/or local therapy. It is possible that both modalities might be inherently limited in the setting of post-prostatectomy with low PSAs, for which more research data is needed. We think, when coupled with mpMRI, PSMA-based ^{18}F-DCFPyL PET/CT could increase diagnostic confidence in the detection of recurrent disease within the prostate bed.

Acknowledgements

We thank Mr. Hui (Hugh) Song's help in data collection.

Disclosure of conflict of interest

None.

Address correspondence to: Dr. Yang Lu, Department of Nuclear Medicine, Division of Diagnostic Imaging, The University of Texas MD Anderson Cancer Center, 1400 Pressler St. Unit 1483, Houston, TX 77030, United States. E-mail: ylu10@mdanderson.org

References

[1] Siegel RL, Miller KD and Jemal A. Cancer statistics, 2017. CA Cancer J Clin 2017; 67: 7-30.

[2] Bray F, Ferlay J, Soerjomataram I, Siegel RL, Torre LA and Jemal A. Global cancer statistics 2018: GLOBOCAN estimates of incidence and mortality worldwide for 36 cancers in 185 countries. CA Cancer J Clin 2018; 68: 394-424.

[3] Silver DA, Pellicer I, Fair WR, Heston WD and Cordon-Cardo C. Prostate-specific membrane antigen expression in normal and malignant human tissues. Clin Cancer Res 1997; 3: 81-85.

[4] Hofman MS, Hicks RJ, Maurer T and Eiber M. Prostate-specific membrane antigen PET: clinical utility in prostate cancer, normal patterns, pearls, and pitfalls. Radiographics 2018; 38: 200-217.

[5] Chang SS, Reuter VE, Heston WD, Bander NH, Grauer LS and Gaudin PB. Five different anti-prostate-specific membrane antigen (PSMA) antibodies confirm PSMA expression in tumor-associated neovasculature. Cancer Res 1999; 59: 3192-3198.

[6] Mhawech-Fauceglia P, Zhang S, Terracciano L, Sauter G, Chadhuri A, Herrmann FR and Penetrante R. Prostate-specific membrane antigen (PSMA) protein expression in normal and neoplastic tissues and its sensitivity and specificity in prostate adenocarcinoma: an immunohistochemical study using mutiple tumour tissue microarray technique. Histopathology 2007; 50: 472-483.

[7] Pienta KJ, Gorin MA, Rowe SP, Carroll PR, Pouliot F, Probst S, Saperstein L, Preston MA, Alva AS, Patnaik A, Durack JC, Stambler N, Lin T, Jensen J, Wong V, Siegel BA and Morris MJ. A phase 2/3 prospective multicenter study of the diagnostic accuracy of prostate specific membrane antigen PET/CT with (18)F-DCFPyL in prostate cancer patients (OSPREY). J Urol 2021; 206: 52-61.

[8] Sonni I, Felker ER, Lenis AT, Sisk AE, Bahri S, Allen-Auerbach M, Armstrong WR, Suvannarerg V, Tubtawee T, Grogan T, Elashoff D, Eiber M, Raman SS, Czernin J, Reiter RE and Calais J. Head-to-head comparison of (68)Ga-PSMA-11 PET/CT and mpMRI with a histopathology gold standard in the detection, intraprostatic localization, and determination of local extension of primary prostate cancer: results from a prospective single-center imaging trial. J Nucl Med 2022; 63: 847-854.

[9] Spohn S, Jaegle C, Fassbender TF, Sprave T, Gkika E, Nicolay NH, Bock M, Ruf J, Benndorf

M, Gratzke C, Grosu AL and Zamboglou C. Intraindividual comparison between (68)Ga-PSMA-PET/CT and mpMRI for intraprostatic tumor delineation in patients with primary prostate cancer: a retrospective analysis in 101 patients. Eur J Nucl Med Mol Imaging 2020; 47: 2796-2803.

[10] Çelen S, Gültekin A, Özlülerden Y, Mete A, Sağtaş E, Ufuk F, Yüksel D, Yağcı B and Zümrütbaş AE. Comparison of 68Ga-PSMA-I/T PET-CT and multiparametric MRI for locoregional staging of prostate cancer patients: a pilot study. Urol Int 2020; 104: 684-691.

[11] Afshar-Oromieh A, Vollnberg B, Alberts I, Bähler A, Sachpekidis C, Dijkstra L, Haupt F, Boxler S, Gross T, Holland-Letz T, Thalmann G, Heverhagen J, Rominger A, Härmä K and Maurer MH. Comparison of PSMA-ligand PET/CT and multiparametric MRI for the detection of recurrent prostate cancer in the pelvis. Eur J Nucl Med Mol Imaging 2019; 46: 2289-2297.

[12] Berger I, Annabattula C, Lewis J, Shetty DV, Kam J, Maclean F, Arianayagam M, Canagasingham B, Ferguson R, Khadra M, Ko R, Winter M, Loh H and Varol C. (68)Ga-PSMA PET/CT vs. mpMRI for locoregional prostate cancer staging: correlation with final histopathology. Prostate Cancer Prostatic Dis 2018; 21: 204-211.

[13] Freitag MT, Radtke JP, Afshar-Oromieh A, Roethke MC, Hadaschik BA, Gleave M, Bonekamp D, Kopka K, Eder M, Heusser T, Kachelriess M, Wieczorek K, Sachpekidis C, Flechsig P, Giesel F, Hohenfellner M, Haberkorn U, Schlemmer HP and Dimitrakopoulou-Strauss A. Local recurrence of prostate cancer after radical prostatectomy is at risk to be missed in (68)Ga-PSMA-11-PET of PET/CT and PET/MRI: comparison with mpMRI integrated in simultaneous PET/MRI. Eur J Nucl Med Mol Imaging 2017; 44: 776-787.

[14] Fay MP. Two-sided exact tests and matching confidence intervals for discrete data. The R Journal 2010; 2: 5.

[15] Zhou C, Tang Y, Deng Z, Yang J, Zhou M, Wang L and Hu S. Comparison of (68)Ga-PSMA PET/CT and multiparametric MRI for the detection of low- and intermediate-risk prostate cancer. EJNMMI Res 2022; 12: 10.

[16] Tanaka T, Yang M, Froemming AT, Bryce AH, Inai R, Kanazawa S and Kawashima A. Current imaging techniques for and imaging spectrum of prostate cancer recurrence and metastasis: a pictorial review. Radiographics 2020; 40: 709-726.

[17] Eiber M, Maurer T, Souvatzoglou M, Beer AJ, Ruffani A, Haller B, Graner FP, Kübler H, Haberkorn U, Eisenhut M, Wester HJ, Gschwend JE and Schwaiger M. Evaluation of hybrid 68Ga-PSMA ligand PET/CT in 248 patients with biochemical recurrence after radical prostatectomy. J Nucl Med 2015; 56: 668-674.

[18] Rahbar K, Ahmadzadehfar H, Seifert R and Boegemann M. [(177)Lu]-PSMA-617 radionuclide therapy in patients with metastatic castration-resistant prostate cancer. Lancet Oncol 2018; 19: e371.

[19] Chakraborty PS, Tripathi M, Agarwal KK, Kumar R, Vijay MK and Bal C. Metastatic poorly differentiated prostatic carcinoma with neuroendocrine differentiation: negative on 68Ga-PSMA PET/CT. Clin Nucl Med 2015; 40: e163-166.

[20] Lopes Dias J, Lucas R, Magalhães Pina J, João R, Costa NV, Leal C, Bilhim T, Campos Pinheiro L and Mateus Marques R. Post-treated prostate cancer: normal findings and signs of local relapse on multiparametric magnetic resonance imaging. Abdom Imaging 2015; 40: 2814-2838.

[21] Casciani E, Polettini E, Carmenini E, Floriani I, Masselli G, Bertini L and Gualdi GF. Endorectal and dynamic contrast-enhanced MRI for detection of local recurrence after radical prostatectomy. AJR Am J Roentgenol 2008; 190: 1187-1192.

[22] Nguyen TT, Bhosale PR and Lu Y. 18F-fluciclovine PET detected early tumor recurrence in prostatectomy bed with low PSA of 0.3 ng/ml but negative on 18F-PSMA PET scan. Clin Nucl Med 2023; 48: 69-70.

[23] Grant K, Lindenberg ML, Shebel H, Pang Y, Agarwal HK, Bernardo M, Kurdziel KA, Turkbey B and Choyke PL. Functional and molecular imaging of localized and recurrent prostate cancer. Eur J Nucl Med Mol Imaging 2013; 40 Suppl 1: S48-59.

[24] Hötker AM, Mazaheri Y, Zheng J, Moskowitz CS, Berkowitz J, Lantos JE, Pei X, Zelefsky MJ, Hricak H and Akin O. Prostate cancer: assessing the effects of androgen-deprivation therapy using quantitative diffusion-weighted and dynamic contrast-enhanced MRI. Eur Radiol 2015; 25: 2665-2672.

[25] Rouvière O, Vitry T and Lyonnet D. Imaging of prostate cancer local recurrences: why and how? Eur Radiol 2010; 20: 1254-1266.

[26] Venkatesan AM, Stafford RJ, Duran C, Soni PD, Berlin A and McLaughlin PW. Prostate magnetic resonance imaging for brachytherapists: anatomy and technique. Brachytherapy 2017; 16: 679-687.

[27] Valle LF, Greer MD, Shih JH, Barrett T, Law YM, Rosenkrantz AB, Shebel H, Muthigi A, Su D, Merino MJ, Wood BJ, Pinto PA, Krauze AV,

Kaushal A, Choyke PL, Türkbey B and Citrin DE. Multiparametric MRI for the detection of local recurrence of prostate cancer in the setting of biochemical recurrence after low dose rate brachytherapy. Diagn Interv Radiol 2018; 24: 46-53.

[28] de Galiza Barbosa F, Queiroz MA, Nunes RF, Costa LB, Zaniboni EC, Marin JFG, Cerri GG and Buchpiguel CA. Nonprostatic diseases on PSMA PET imaging: a spectrum of benign and malignant findings. Cancer Imaging 2020; 20: 23.